Nano Research

Open Access

Research Article

Carbon-supported CeNCl as an efficient catalyst for CO_2 cycloaddition

Li Liu[1,2], Lingling Zhang[2], Xiang Chu[1,2], Baokang Geng[1,2], Huilin Wang[2], Zongxiang Li[3], Xiao Wang[1,2] ✉, Shuyan Song[1,2] ✉, and Hongjie Zhang[1,2,4] ✉

[1] *School of Applied Chemistry and Engineering, University of Science and Technology of China, Hefei 230026, China*
[2] *State Key Laboratory of Rare Earth Resource Utilization, Changchun Institute of Applied Chemistry, Chinese Academy of Sciences, Changchun 130022, China*
[3] *Sinocare Incorporation, Changsha 410221, China*
[4] *Department of Chemistry, Tsinghua University, Beijing 100084, China*

Cite this article: *Nano Research*, **2025**, *18*, 94907028. https://doi.org/10.26599/NR.2025.94907028

ABSTRACT: The cycloaddition reaction of CO_2 with epoxide not only effectively reduces the concentration of CO_2 in the atmosphere, but also has excellent industrial application value and up to 100% atom utilization, but there are difficulties in separation and recovery of traditional homogeneous catalysts, harsh reaction conditions of traditional heterogeneous catalysts, and activation of CO_2 molecules. In this paper, an easily synthesized heterogeneous catalyst CeNCl/C was used to catalyze the cycloaddition reaction of CO_2 with styrene oxide, with a high yield of 92.7%, a high selectivity of 96.7%, a turnover numbers (TON) value of 349, and a good stability demonstrated in six cycle tests (equivalent to 216 h of testing). Through comprehensive studies, it was shown that CeNCl/C contains Lewis acid-base centers as active centers, which can effectively reduce the energy barrier required for ring opening of the reaction substrate, enhance the adsorption and activation of CO_2, and promote the formation of intermediates, which led to the acquisition of excellent catalytic activity.

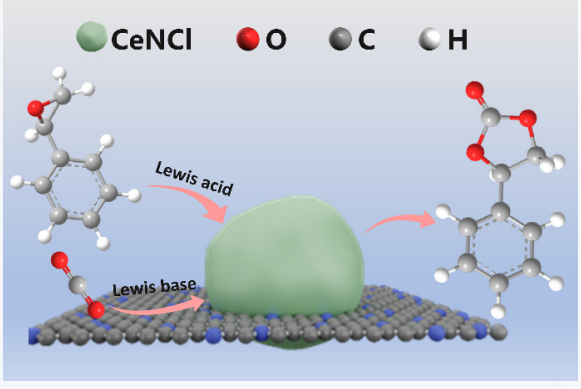

KEYWORDS: CO_2 cycloaddition, heterogeneous catalysis, CeNCl, Lewis acid/base

1 Introduction

As a major component of exhaust gases from fossil fuel consumption, excessive CO_2 emissions exacerbate the greenhouse effect and pose a serious threat to ecosystems [1, 2]. Synthesis of high-value-added chemicals with CO_2 has the potential to control carbon dioxide emissions and reduce dependence on fossil resources. One of the most effective strategies for CO_2 conversion is the cycloaddition reaction between CO_2 and epoxides to generate cyclic carbonates [3]. From the point of view of green and sustainable chemistry, cycloaddition reactions have a broad and vital industrial application value since this transformation pathway not only makes 100% atom utilisation but also generates cyclic carbonates, which are essential intermediates in pharmaceuticals and fine chemicals, components of battery electrolytes, precursors of polycarbonate materials and polar solvents that are inert to protons [4–8]. However, the CO_2 molecule is very stable (the standard formation Gibbs free energy (ΔG_f) = 394.228 kJ·mol^{-1}) and the C atom therein is at its most stable valence (IV) [9]. Therefore, the conversion of CO_2 to other products requires the use of catalysts and highly reactive co-reactants. A large number of catalysts have been developed for CO_2 cycloaddition reactions, including homogeneous and heterogeneous catalysts [10–12]. Homogeneous catalysts include ionic liquids, metal complexes and porous polymers [13–16]. However, the synthesis complexity, separation and recovery difficulty, harsh reaction conditions and expensive monomers of homogeneous catalysts have limited their large-scale industrial applications [10, 17, 18]. In comparison, heterogeneous catalysts (e.g., molecular sieves, metal-organic skeletons and mesoporous oxides) usually have stable structures, which can effectively overcome the problems of difficult separation

Received: July 24, 2024; **Revised:** September 1, 2024
Accepted: September 10, 2024

✉Address correspondence to Xiao Wang, wangxiao@ciac.ac.cn; Shuyan Song, songsy@ciac.ac.cn; Hongjie Zhang, hongjie@ciac.ac.cn

and recovery of homogeneous catalysts and are expected to be industrially available, but they usually require appropriate high temperature and high pressure (> 120 °C and 3 MPa) to drive the reactions [19–22]. Therefore, taking into account energy and cost, it is necessary to develop green technology to synthesise easily separated heterogeneous catalysts to promote the cycloaddition reaction between CO_2 and epoxides under mild reaction conditions.

The general mechanism of the cycloaddition reaction catalyzed by acid-base bifunctional catalysts is well known. The ring-opening of epoxides involves the adsorption of reactants and the cleavage of the C–O bond [23]. Among them, the Lewis acid can coordinate with the O atom in the epoxy ring to decrease the energy barrier for ring opening and at the same time form a good leaving group to accelerate the breakage of the C–O bond [24, 25]. In addition, the Lewis base can activate the CO_2 molecule [26]. Therefore, catalyst systems in which Lewis acid and Lewis base coexist can effectively promote the reaction. CeO_2 is a cheap and readily available metal oxide that possesses both Lewis acid and base sites and exhibits good catalytic activity for CO_2 cycloaddition reactions [27, 28]. However, existing CeO_2-based catalysts for CO_2 cycloaddition reactions typically require high temperatures over 150 °C and high pressures above 5 MPa [29, 30]. Therefore, we envisage further reducing the energy required during the reaction by adjusting the strength of the Lewis acid-base sites in the cerium-based catalysts.

In this work, we obtained carbon-supported CeNCl (CeNCl/C) by ball milling-calcination method. Subsequently, we applied CeNCl/C to the cycloaddition reaction of styrene oxide (SO) and CO_2 and achieved a 92.7% yield of styrene carbonate (SC) with 96.7% selectivity and a turnover numbers (TON) value of 349. Even more impressive is that after 216 h of 6-cycle testing, it maintained 90% of the initial SC yield. The CeNCl/C material has both Lewis acid-base active centers, which improves the ability to trap CO_2 and activate styrene oxide. Also, it exhibits a stable chemical structure and excellent catalytic performance, which has great potential for application and provides an idea for designing and developing heterogeneous catalysts for efficiently utilising CO_2.

2 Results and discussion

2.1 Synthesis and characterization

The schematic diagram of CeNCl/C catalyst preparation by ball milling-calcination method is shown in Fig. 1(a). Firstly, anhydrous $CeCl_3$ was homogeneously dispersed on chitosan carriers by ball milling. Then, the mixture was calcined under N_2 at 800 °C for 2 h to obtain black powder. The same procedure synthesized CeO_2/C and C carriers unloaded with Ce species. Scanning electron microscopy (SEM) and transmission electron microscopy (TEM) images were used to observe the morphology of these as-prepared catalysts (Figs. S1 and S2 in the Electronic Supplementary Material (ESM)). There is no noticeable difference in the morphology of the catalysts. High-resolution TEM (HR-TEM) images show a uniform comparative distribution of CeNCl on the carbon carrier in CeNCl/C, the lattice fringes of 0.29 nm could be attributed to the (110) crystal planes of CeNCl (Figs. 1(b) and 1(c)), which was also confirmed by the selective area electron diffraction (SAED) image (Fig. S3 in the ESM). CeO_2 in CeO_2/C is distributed as nanoparticles on the carrier and HR-TEM images show a lattice stripe of 0.191 nm, corresponding to the (220) crystal plane of CeO_2 (Figs. 1(e) and 1(f)). The energy-dispersive X-ray (EDX) element mapping of CeNCl/C and CeO_2/C exhibited that Ce, N, Cl and Ce, O elements are each uniformly distributed (Figs. 1(d) and 1(g)).

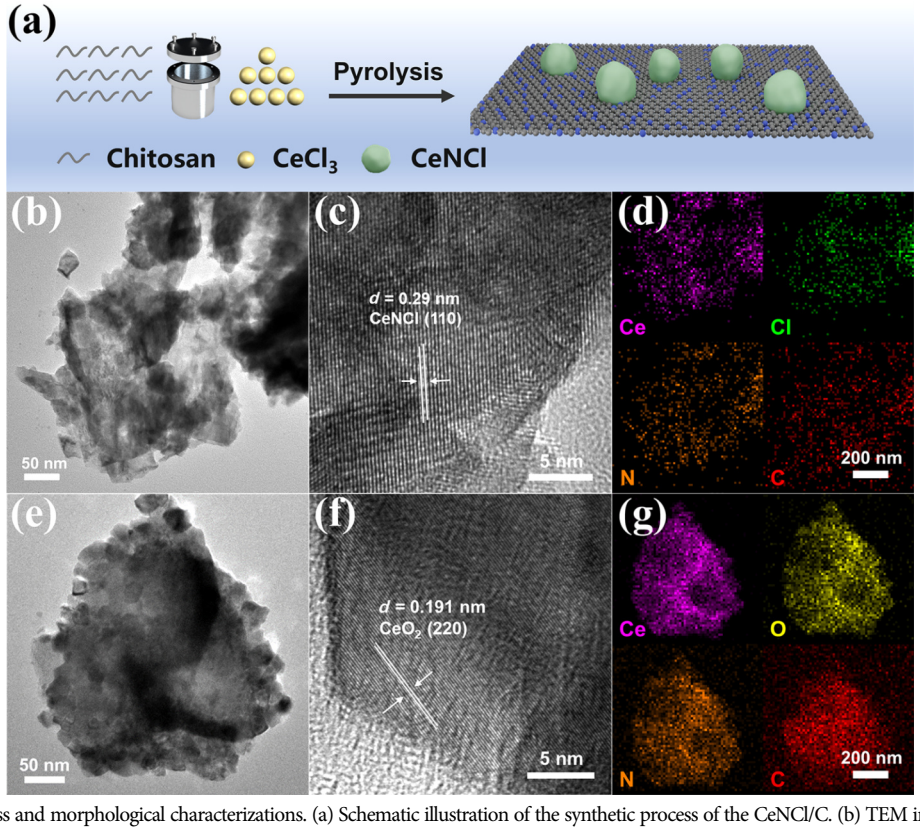

Figure 1 Synthesis process and morphological characterizations. (a) Schematic illustration of the synthetic process of the CeNCl/C. (b) TEM image, (c) HR-TEM image, and (d) the corresponding element mapping images of CeNCl/C. (e) TEM image, (f) HR-TEM image, and (g) the corresponding element mapping images of CeO_2/C.

The X-ray diffraction (XRD) pattern in Fig. 2(a) of CeNCl/C and CeO_2/C shows sharp peaks at 12.9°, 25.4°, 30.9° and 34.2° in CeNCl/C, corresponding to the (001), (101), (110) and (102) planes of CeNCl (PDF #49-1578) [31]. Similarly, the presence of three peaks at 28.5°, 33.1° and 47.4° in CeO_2/C correspond to the (111), (200) and (220) planes (PDF #34-0397). To elucidate the surface and composition of the catalysts, we performed X-ray photoelectron spectroscopy (XPS) measurements. Figure 2(b) shows the XPS Ce 3d spectra of CeNCl/C and CeO_2/C. The Ce 3d spectral peaks are fitted into 8 peaks according to their binding energies, corresponding to Ce $3d_{5/2}$ and Ce $3d_{3/2}$. Among them, V' (885.1 eV) and U' (905.1 eV) represent a Ce $3d_{5/2}$ peak and a Ce $3d_{3/2}$ peak in the Ce 3d XPS spectrum are attributed to Ce^{3+} while others correspond to Ce^{4+} [32, 33]. The calculated surface Ce^{4+} concentration of CeNCl/C is 77.5%, which is much higher than that of CeO_2/C (64.1%) (Table S2 in the ESM), indicating that more Ce species in CeNCl/C exist as the more Lewis acidic Ce^{4+}. The N 1s spectrum in Fig. 2(c) contains peaks at 398.0, 399.5 and 400.5 eV, originating from pyridinic N, pyrrolic N and graphitic N [34, 35]. The content of pyridinic N that can be used as a Lewis base site in CeNCl/C and CeO_2/C is 32.34% and 26.11%, respectively. In addition, the Cl 2p spectrum of CeNCl/C shows that the Cl element exists in the lattice Cl^- (Fig. S5 in the ESM). The Raman spectra of CeNCl/C and CeO_2/C have two unique peaks at around 1350 cm^{-1} (D band) and 1590 cm^{-1} (G band), and their intensities are represented by I_D and I_G respectively. The intensity ratio of these two peaks (I_D/I_G) for CeNCl/C (0.98) was higher than that of CeO_2/C (0.82), suggesting that the CeNCl/C possessed more defects than the CeO_2/C (Fig. 2(d)) [36]. The surface area and pore characteristics of CeNCl/C and CeO_2/C were determined by N_2 adsorption/desorption and the results are shown in Fig. S6 and Table S4 in the ESM. CeNCl/C and CeO_2/C showed type-IV N_2 adsorption–desorption isotherm, indicating their mesoporous properties. The Brunauer–Emmett–Teller (BET) surface areas of CeNCl/C and CeO_2/C were 18.13 and 15.12 $m^2 \cdot g^{-1}$, respectively, but their pore size distributions and pore volumes were close. Therefore, CeNCl/C may be more favorable than CeO_2/C for improving mass diffusion.

2.2 Catalytic performance

Among various cyclic carbonates, SC generated by the cycloaddition of SO and CO_2 has attracted widespread attention, with the market capitalization of SC approximately 120 times that of SO [37]. We evaluated and compared the catalytic activity of the catalysts for the formation of SC from SO using N,N-dimethylformamide (DMF) as solvent and tetrabutylammonium bromide (t-TBAB) as co-catalyst. The effects of temperature, CO_2 pressure and catalyst dosage on the reaction were investigated to optimise the reaction conditions. The effect of temperature is relatively significant. The yield increased rapidly from 6.7% to 38.1% after 12 h of reaction as the temperature increased from 70 to 80 °C and the highest yield was reached at 100 °C. When the temperature is 110 °C, the yield shows a downward trend because the target product's selectivity decreases (Fig. S7(a) in the ESM). A similar trend was observed for the pressure of CO_2. The yield at the initial pressure of 1.0 MPa was more significant than that at 0.5 MPa and atmospheric pressure was close to that at 1.5 MPa. However, the yield and selectivity decreased at an initial reaction pressure of 2.0 MPa, which was attributed to the promotion of the reaction by-products after increasing the pressure (Fig. S7(b) in the ESM). In addition, when the mass of the catalyst was increased in the range of 0–50 mg the yield continued to increase, but when the mass reached 75 mg, a decrease in the reaction yield was observed. This may be because the excess catalyst is not conducive to mass transfer during the reaction (Fig. S7(c) in the ESM). Additionally, the other types of solvents and quaternary ammonium salts were also studied and compared (Figs. S7(d) and S7(e) in the ESM). Therefore, 50 mg of CeNCl/C was used for further reactions under relatively mild conditions of 100 °C and 1.0 MPa CO_2.

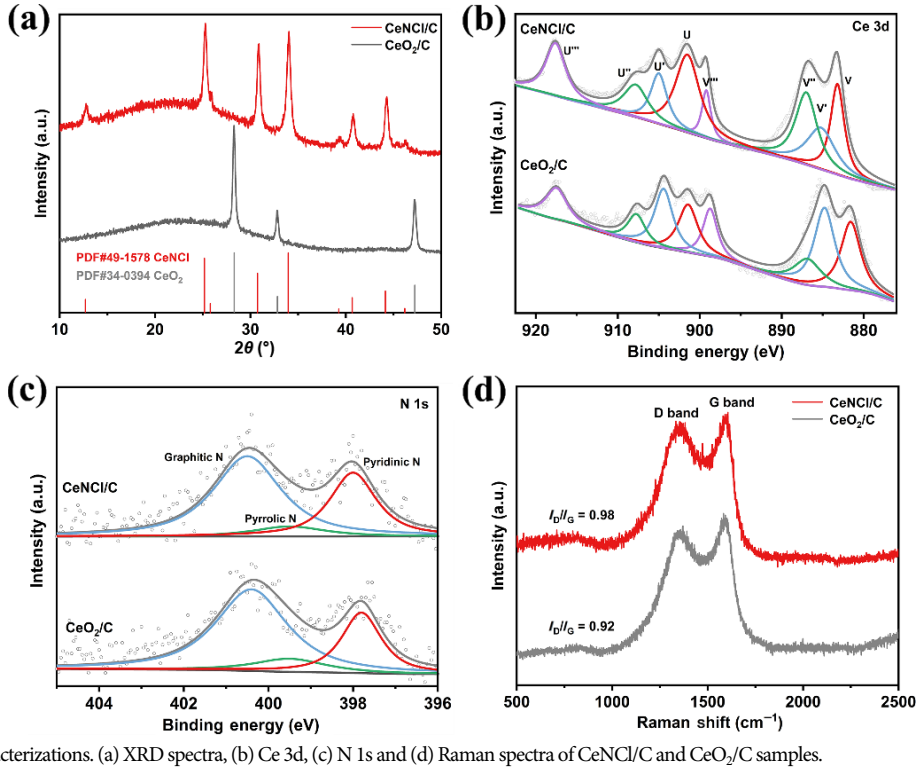

Figure 2 Structural characterizations. (a) XRD spectra, (b) Ce 3d, (c) N 1s and (d) Raman spectra of CeNCl/C and CeO_2/C samples.

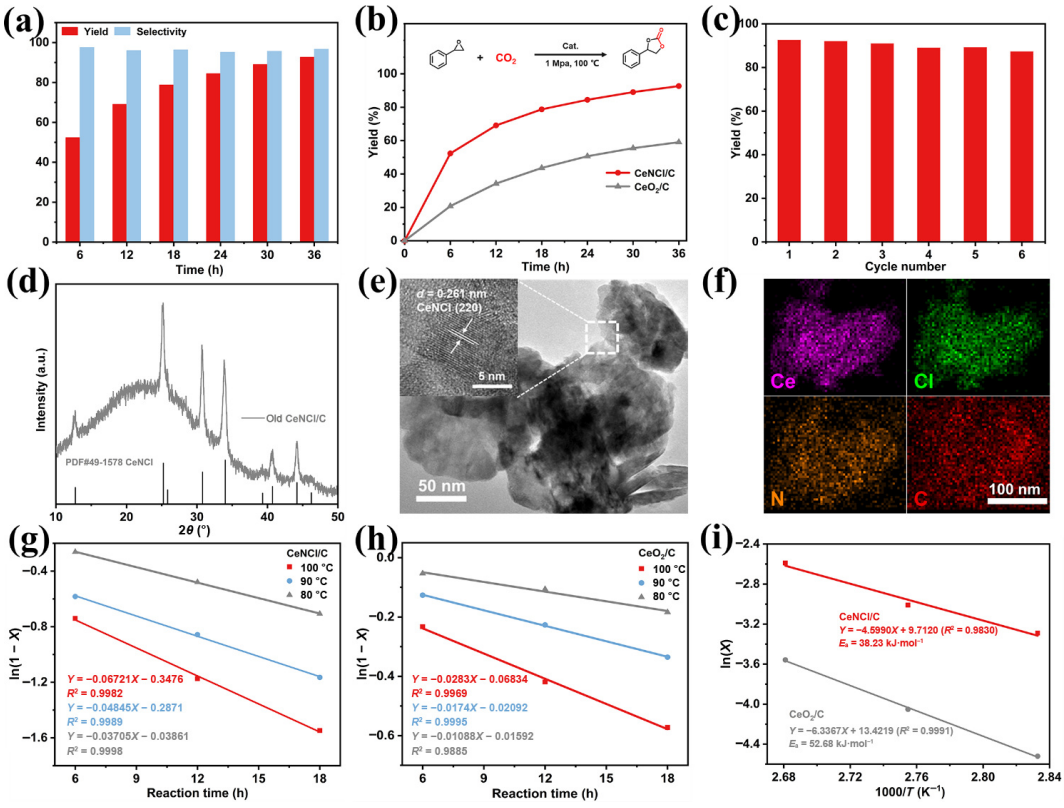

Figure 3 Catalytic performances. (a) SC yield and selectivity of CeNCl/C after reacting for 36 h, (b) SC yields of CeNCl/C and CeO_2/C for different reaction times, (c) SC yields of CeNCl/C at different cycles each for 36 h. (d) XRD spectrum, (e) HR-TEM image, and (f) the corresponding element mapping images of CeNCl/C after cyclic expriments. (g) and (h) First order reaction rate plots and (i) Arrhenius plots for CeNCl/C and CeO_2/C at 100 °C (red), 90 °C (blue) and 80 °C (grey).

Figure 3(a) shows the time dependence of yield and selectivity in CeNCl/C-catalyzed cycloaddition of CO_2. After 36 h of reaction, the yield of CeNCl/C reached 92.7%, the SC selectivity was 96.7% and the TON value reached 349, indicating its excellent catalytic activity for CO_2 cycloaddition. As shown in Fig. 3(b) and Fig. S8 in the ESM, the yield of CeNCl/C was much higher than those of CeO_2/C (59.1%) and C carrier (17.3%) under the same experimental conditions and there was almost no cycloaddition reaction occurring in the absence of catalysts and co-catalysts. Furthermore, in the absence of CeNCl/C or t-TBAB, the target product was reduced, suggesting that both are necessary for the CO_2 cycloaddition reaction. The catalytic activity of CeNCl/C is also better than most previously reported catalysts (Table S6 in the ESM). One of the biggest advantages of heterogeneous catalysts is the ease of separation and recovery from the reaction mixture. Therefore, we further studied the recovery and recyclability of CeNCl/C. After a cycle of 36 h reaction at 100 °C, the catalyst was recovered, washed, dried and then mixed with fresh SO and DMF for subsequent reaction cycles. As shown in Fig. 3(c), it can maintain more than 90% of the initial catalytic yield after 6 cycles (equivalent to 216 h of testing). The crystal structure and morphology of CeNCl/C remained well maintained after 6 cycles (Figs. 3(d)–3(f)). The proportion of Ce^{4+} in the catalysts can also be maintained stably after the reaction (Fig. S9 and Table S7 in the ESM), indicating that the CeNCl/C is structurally stable and has good recyclability in the reaction of CO_2 with SO. Furthermore, we demonstrated the ability of CeNCl/C to catalyze the cycloaddition of CO_2 with other epoxides (Table 1) and most epoxides could be converted to the corresponding cyclic carbonates with high yields,

Table 1 Cycloaddition of CO_2 with various epoxides[ab]

Entry	Epoxide	Product	Yield	TON
1			92.65%	349.3
2			96.7%	541.8
3			96.5%	601.8
4			89.4%	448.4
5			85.8%	364.5
6			57.1%	279.3
7			92.0%	440.7
8			92.8%	439.1
9		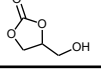	79.5%	509.5

[a]Reaction conditions: 2.5 mL epoxide, 1 MPa CO_2, 100 °C, 36 h, 50 mg catalyst, 5 mg TBAB. [b]Data were acquired based on gas chromatography-mass spectrometry (GC-MS) analysis.

suggesting that the ability to catalyze this type of reaction is universal. Notably, under the same reaction conditions, higher yields of carbonate products can be obtained from small-sized epoxides compared to larger epoxides, which may be due to the spatial site-barrier effect of the large-sized substituents [38]. To further study the different catalytic efficiencies of CeNCl/C and CeO_2/C, the kinetics of the cycloaddition reaction of SO and CO_2 were studied at 80, 90 and 100 °C (other conditions unchanged). As shown in Figs. 3(g)–3(i), the catalytic activities of CeNCl/C and CeO_2/C increase with the reaction temperature increase. At the same reaction temperature, the reaction rate of CeNCl/C is at least 2.4 times that of CeO_2/C. Based on the above kinetic results, the activation energies of various catalysts were further calculated using the Arrhenius equation [39]. As shown in Fig. 3(i), the activation energy of CeNCl/C is 38.23 kJ·mol^{-1}, much lower than the activation energy of CeO_2/C (52.68 kJ·mol^{-1}). These results also show CeNCl/C has higher energy efficiency than CeO_2/C.

2.3 Reaction mechanism

NH_3-TPD (TPD: temperature programmed desorption) and CO_2-TPD further confirmed the Lewis acid-base active sites in the catalyst. For Lewis acid/base sites, the desorption peaks can be divided into weak, intermediate and strong sites, corresponding to desorption temperatures at < 473 K, 473–673 K and > 673 K, in that order [40, 41]. The CO_2-TPD results are shown in Fig. 4(a), the intensity of the CO_2 adsorption peaks on CeNCl/C are greater and shift to a higher temperature, indicating that the proportion of strong Lewis base sites in CeNCl/C increases significantly compared with CeO_2/C. Similar adsorption differences were also observed in NH_3-TPD measurements (Fig. 4(b)), indicating a higher density of Lewis acid sites in CeNCl/C. This is consistent with the Ce 3d XPS results of the catalyst. Therefore, we speculate that pyridinic N and Ce^{4+} in CeNCl/C serve as Lewis acid/base sites respectively, making CeNCl/C more conducive to promoting the CO_2 cycloaddition reaction [42–44]. Another critical factor affecting the performance of CO_2 cycloaddition is the adsorption capacity of the catalysts for CO_2. We tested the CO_2 adsorption isotherms of CeNCl/C and CeO_2/C (Fig. 4(c)) and the faster and more rapid uptake of CO_2 by CeNCl/C compared to CeO_2/C confirms that CeNCl/C has a greater affinity for CO_2. Previous reports proposed a possible reaction mechanism for CO_2 cycloaddition using CeNCl/C as a catalyst [45, 46], as shown in Fig. 4(d). CO_2 and epoxides are adsorbed on the Lewis acid-base sites of the catalyst and a "Ce-O" adduct is formed between the Lewis acidic Ce site and the O atom of SO, thus activating the C–O bond. Simultaneously, the Br^- of TBAB will attack the less sterically hindered C atom in the three-membered ring of SO and promote its ring opening, which is generally considered the rate-controlling step of the cycloaddition reaction. Subsequently, the O^- in the activated CO_2 attacks the C atom coordinated to Br^- and the C atom of the activated CO_2 reacts with the ring-opening epoxide. Finally, the Br^- is released and the ring is closed to form a cyclic carbonate product.

3 Conclusions

In summary, we successfully prepared a carbon-supported CeNCl catalyst through the ball milling-calcination method. The Ce site with a Lewis acid centre generates CeNCl by combining the surrounding N atoms with Lewis basicity. The acid-base sites cooperate to promote the activation of the substrate. The results show CeNCl/C exhibits excellent catalytic activity in the CO_2 cycloaddition reaction under mild conditions due to the strong interaction between its Lewis acid and base sites. This work designed and synthesized a CO_2 cycloaddition heterogeneous catalyst with excellent performance and also explained the operating mechanism of multiple active sites in CO_2 conversion.

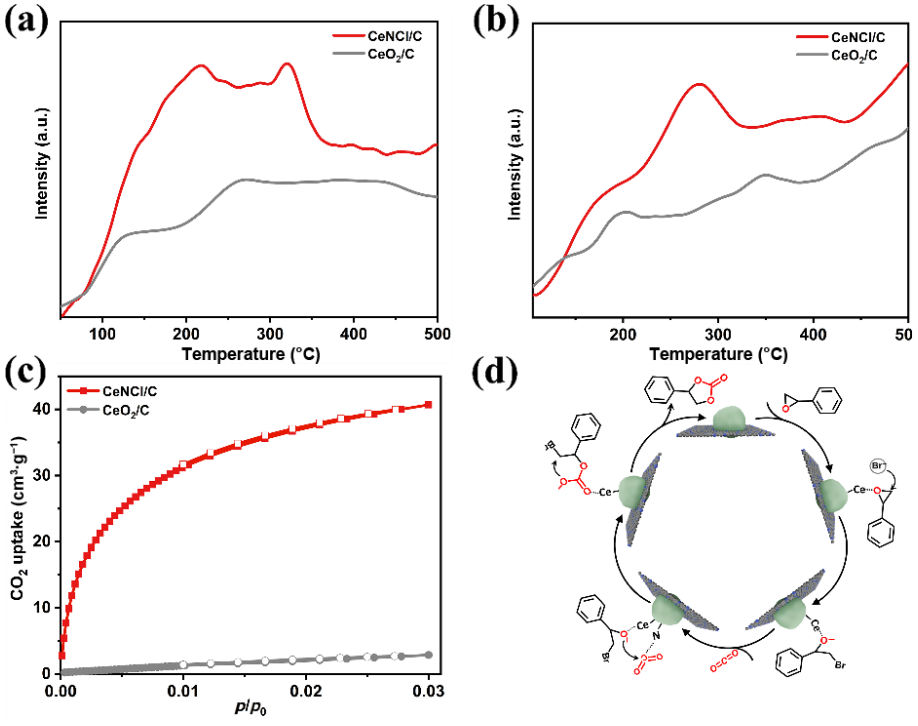

Figure 4 (a) CO_2-TPD profiles, (b) NH_3-TPD profiles and (c) CO_2 adsorption–desorption profiles of CeNCl/C and CeO_2/C. (d) A plausible mechanism for the cycloaddition of SO with CO_2 over CeNCl/C.

Electronic Supplementary Material: Supplementary material (details of catalysts preparation, characterizations, electrochemical measurements, Figs. S1–S9 and Tables S1–S7) is available in the online version of this article at https://doi.org/10.26599/NR.2025.94907028.

Data availability

All data needed to support the conclusions in the paper are presented in the manuscript and the Electronic Supplementary Material. Additional data related to this paper may be requested from the corresponding author upon request.

Acknowledgements

This work was supported by the financial aid from the National Key Research and Development Program of China (No. 2021YFB3500700), the National Natural Science Foundation of China (Nos. 22020102003, 22025506, 22271274 and U23A20140), Jilin Province Science and Technology Development Plan Project (No. 20230101022JC) and Hunan Province High-tech Industry Science and Technology Innovation Leading Plan (No. 2022GK4021). X. W. acknowledges funding from National Natural Science Foundation of China Outstanding Youth Science Foundation of China (Overseas).

Declaration of competing interest

All the contributing authors declare no conflict of interest in this work.

Author contribution statement

All the authors have approved the final manuscript.

Use of AI statement

None.

References

[1] Wu, P. Y.; Li, Y.; Zheng, J. J.; Hosono, N.; Otake, K. I.; Wang, J.; Liu, Y. H.; Xia, L. L.; Jiang, M.; Sakaki, S. et al. Carbon dioxide capture and efficient fixation in a dynamic porous coordination polymer. *Nat. Commun.* **2019**, *10*, 4362.

[2] Gao, W. Y.; Chen, Y.; Niu, Y. H.; Williams, K.; Cash, L.; Perez, P. J.; Wojtas, L.; Cai, J. F.; Chen, Y. S.; Ma, S. Q. Crystal engineering of an nbo topology metal-organic framework for chemical fixation of CO_2 under ambient conditions. *Angew. Chem., Int. Ed.* **2014**, *53*, 2615–2619.

[3] Zhu, J. J.; Diao, T. T.; Wang, W. Y.; Xu, X. L.; Sun, X. Y.; Carabineiro, S. A. C.; Zhao, Z. Boron doped graphitic carbon nitride with acid-base duality for cycloaddition of carbon dioxide to epoxide under solvent-free condition. *Appl. Catal. B: Environ.* **2017**, *219*, 92–100.

[4] Yang, Q. H.; Yang, C. C.; Lin, C. H.; Jiang, H. L. Metal-organic-framework-derived hollow N-doped porous carbon with ultrahigh concentrations of single Zn atoms for efficient carbon dioxide conversion. *Angew. Chem., Int. Ed.* **2019**, *58*, 3511–3515.

[5] Shaikh, R. R.; Pornpraprom, S.; D'Elia, V. Catalytic strategies for the cycloaddition of pure, diluted, and waste CO_2 to epoxides under ambient conditions. *ACS Catal.* **2018**, *8*, 419–450.

[6] Zhou, Z.; He, C.; Xiu, J.; Yang, L.; Duan, C. Y. Metal-organic polymers containing discrete single-walled nanotube as a heterogeneous catalyst for the cycloaddition of carbon dioxide to epoxides. *J. Am. Chem. Soc.* **2015**, *137*, 15066–15069.

[7] Li, P. Z.; Wang, X. J.; Liu, J.; Lim, J. S.; Zou, R. Q.; Zhao, Y. L. A triazole-containing metal-organic framework as a highly effective and substrate size-dependent catalyst for CO_2 conversion. *J. Am. Chem. Soc.* **2016**, *138*, 2142–2145.

[8] Wang, T.; Zhu, Y. Q.; Wang, W.; Niu, J. F.; Lu, Z. Y.; He, P. L. Polyoxometalates coupled covalent organic frameworks as highly active photothermal nanoreactor for CO_2 cycloaddition. *Nano Res.* **2024**, *17*, 5975–5984.

[9] Claver, C.; Yeamin, M. B.; Reguero, M.; Masdeu-Bultó, A. M. Recent advances in the use of catalysts based on natural products for the conversion of CO_2 into cyclic carbonates. *Green Chem.* **2020**, *22*, 7665–7706.

[10] Pal, T. K.; De, D.; Bharadwaj, P. K. Metal-organic frameworks for the chemical fixation of CO_2 into cyclic carbonates. *Coord. Chem. Rev.* **2020**, *408*, 213173.

[11] Yan, T.; Liu, H.; Zeng, Z. X.; Pan, W. G. Recent progress of catalysts for synthesis of cyclic carbonates from CO_2 and epoxides. *J. CO_2 Util.* **2023**, *68*, 102355.

[12] Saptal, V. B.; Bhanage, B. M. Current advances in heterogeneous catalysts for the synthesis of cyclic carbonates from carbon dioxide. *Curr. Opin. Green Sustain. Chem.* **2017**, *3*, 1–10.

[13] Zhang, Y. Y.; Yang, G. W.; Xie, R.; Yang, L.; Li, B.; Wu, G. P. Scalable, durable, and recyclable metal-free catalysts for highly efficient conversion of CO_2 to cyclic carbonates. *Angew. Chem., Int. Ed.* **2020**, *59*, 23291–23298.

[14] Xu, B. H.; Wang, J. Q.; Sun, J.; Huang, Y.; Zhang, J. P.; Zhang, X. P.; Zhang, S. J. Fixation of CO_2 into cyclic carbonates catalyzed by ionic liquids: A multi-scale approach. *Green Chem.* **2015**, *17*, 108–122.

[15] Decortes, A.; Castilla, A. M.; Kleij, A. W. Salen-complex-mediated formation of cyclic carbonates by cycloaddition of CO_2 to epoxides. *Angew. Chem., Int. Ed.* **2010**, *49*, 9822–9837.

[16] Luo, R. C.; Liu, X. Y.; Chen, M.; Liu, B. Y.; Fang, Y. X. Recent advances on imidazolium-functionalized organic cationic polymers for CO_2 adsorption and simultaneous conversion into cyclic carbonates. *ChemSusChem* **2020**, *13*, 3945–3966.

[17] Liu, F. W.; Duan, X. R.; Dai, X.; Du, S. S.; Ma, J. J.; Liu, F. S.; Liu, M. S. Metal-decorated porous organic frameworks with cross-linked pyridyl and triazinyl as efficient platforms for CO_2 activation and conversion under mild conditions. *Chem. Eng. J.* **2022**, *445*, 136687.

[18] Liu, L. N.; Jayakumar, S.; Chen, J.; Tao, L.; Li, H.; Yang, Q. H.; Li, C. Synthesis of bifunctional porphyrin polymers for catalytic conversion of dilute CO_2 to cyclic carbonates. *ACS Appl. Mater. Interfaces* **2021**, *13*, 29522–29531.

[19] Qaroush, A. K.; Alsoubani, F. A.; Al-Khateeb, A. A. M.; Nabih, E.; Al-Ramahi, E.; Khanfar, M. F.; Assaf, K. I.; Eftaiha, A. A. F. An efficient atom-economical chemoselective CO_2 cycloaddition using lanthanum oxide/tetrabutyl ammonium bromide. *Sustain. Energy Fuels* **2018**, *2*, 1342–1349.

[20] Hao, L. D.; Xia, Q. N.; Zhang, Q.; Masa, J.; Sun, Z. Y. Improving the performance of metal-organic frameworks for thermo-catalytic CO_2 conversion: Strategies and perspectives. *Chin. J. Catal.* **2021**, *42*, 1903–1920.

[21] Guillerm, V.; Weseliński, Ł. J.; Belmabkhout, Y.; Cairns, A. J.; D' Elia, V.; Wojtas, Ł.; Adil, K.; Eddaoudi, M. Discovery and introduction of a (3,18)-connected net as an ideal blueprint for the design of metal-organic frameworks. *Nat. Chem.* **2014**, *6*, 673–680.

[22] Yang, D. R.; Wang, X. 2D π-conjugated metal-organic frameworks for CO_2 electroreduction. *SmartMat.* **2022**, *3*, 54–67.

[23] Bobbink, F. D.; Vasilyev, D.; Hulla, M.; Chamam, S.; Menoud, F.; Laurenczy, G.; Katsyuba, S.; Dyson, P. J. Intricacies of cation-anion combinations in imidazolium salt-catalyzed cycloaddition of CO_2 into epoxides. *ACS Catal.* **2018**, *8*, 2589–2594.

[24] Kuang, H. Y.; Lin, Y. X.; Li, X. H.; Chen, J. S. Chemical fixation of CO_2 on nanocarbons and hybrids. *J. Mater. Chem. A* **2021**, *9*, 20857–20873.

[25] Xie, Y.; Wang, T. T.; Liu, X. H.; Zou, K.; Deng, W. Q. Capture and conversion of CO_2 at ambient conditions by a conjugated microporous polymer. *Nat. Commun.* **2013**, *4*, 1960.
[26] Cui, X. J.; Dai, X. C.; Surkus, A. E.; Junge, K.; Kreyenschulte, C.; Agostini, G.; Rockstroh, N.; Beller, M. Zinc single atoms on N-doped carbon: An efficient and stable catalyst for CO_2 fixation and conversion. *Chin. J. Catal.* **2019**, *40*, 1679–1685.
[27] Zhang, S.; Xia, Z. M.; Zou, Y.; Cao, F. X.; Liu, Y. X.; Ma, Y. Y.; Qu, Y. Q. Interfacial frustrated Lewis pairs of CeO_2 activate CO_2 for selective tandem transformation of olefins and CO_2 into cyclic carbonates. *J. Am. Chem. Soc.* **2019**, *141*, 11353–11357.
[28] Xie, Z. H.; Hwang, S.; Chen, J. G. Reduction-induced metal/oxide interfacial sites for selective CO_2 hydrogenation. *SmartMat.* **2023**, *4*, e1201.
[29] Adeleye, A. I.; Patel, D.; Niyogi, D.; Saha, B. Efficient and greener synthesis of propylene carbonate from carbon dioxide and propylene oxide. *Ind. Eng. Chem. Res.* **2014**, *53*, 18647–18657.
[30] Gao, J.; Yue, C. G.; Wang, H.; Li, J. X.; Yao, H.; Wang, M. Y.; Ma, X. B. CeO_2-ZrO_2 solid solution catalyzed and moderate acidic-basic sites dominated cycloaddition of CO_2 with epoxides: Halogen-free synthesis of cyclic carbonates. *Catalysts* **2022**, *12*, 632.
[31] Liu, L.; Wang, F.; Chu, X.; Zhang, L. L.; Zhang, S. S.; Wang, X.; Che, G. B.; Song, S. Y.; Zhang, H. J. CeNCl-CeO_2 heterojunction-modified Ni catalysts for efficient electroreduction of CO_2 to CO. *Adv. Energy Mater.* **2024**, *14*, 2301575.
[32] Zhao, M.; Wang, X.; Xu, J.; Li, Y. O.; Wang, X. M.; Chu, X.; Wang, K.; Wang, Z. J.; Zhang, L. L.; Feng, J. et al. Strengthening the metal-acid interactions by using CeO_2 as regulators of precisely placing Pt species in ZSM-5 for furfural hydrogenation. *Adv. Mater.* **2024**, *36*, 2313596.
[33] Wu, X. T.; Wang, X.; Zhang, L. L.; Wang, X. M.; Song, S. Y.; Zhang, H. J. Polyethylene upgrading to liquid fuels boosted by atomic Ce promoters. *Angew. Chem., Int. Ed.* **2024**, *63*, e202317594.
[34] Wang, S. G.; Qin, J. W.; Zheng, L. R.; Guo, D. L.; Cao, M. H. A self-sacrificing dual-template strategy to heteroatom-enriched porous carbon nanosheets with high pyridinic-N and pyrrolic-N content for oxygen reduction reaction and sodium storage. *Adv. Mater. Interfaces* **2018**, *5*, 1801149.
[35] Li, B. B.; Ju, Z. F.; Zhou, M.; Su, K. Z.; Yuan, D. Q. A reusable MOF-supported single-site zinc(II) catalyst for efficient intramolecular hydroamination of o-alkynylanilines. *Angew. Chem., Int. Ed.* **2019**, *58*, 7687–7691.
[36] Zhu, Z. Z.; Li, Z.; Wei, X. X.; Wang, J. J.; Xiao, S. H.; Li, R.; Wu, R.; Chen, J. S. Achieving efficient electroreduction of CO_2 to CO in a wide potential window by encapsulating Ni nanoparticles in N-doped carbon nanotubes. *Carbon* **2021**, *185*, 9–16.
[37] Rehman, A.; Eze, V. C.; Resul, M. F. M. G.; Harvey, A. Kinetics and mechanistic investigation of epoxide/CO_2 cycloaddition by a synergistic catalytic effect of pyrrolidinopyridinium iodide and zinc halides. *J. Energy Chem.* **2019**, *37*, 35–42.
[38] Dinker, M. K.; Li, M. M.; Zhao, K.; Zuo, M. R.; Ding, L. F.; Liu, X. Q.; Sun, L. B. Transformation of type III to type II porous liquids by tuning surface rigidity of rhodium(II)-based metal-organic polyhedra for CO_2 cycloaddition. *Angew. Chem., Int. Ed.* **2023**, *62*, e202306495.
[39] Aguila, B.; Sun, Q.; Wang, X. L.; O'Rourke, E.; Al-Enizi, A. M.; Nafady, A.; Ma, S. Q. Lower activation energy for catalytic reactions through host–guest cooperation within metal-organic frameworks. *Angew. Chem., Int. Ed.* **2018**, *57*, 10107–10111.
[40] Gupta, N. N.; Punekar, A. S.; Raj, K. R. E. K.; Ghodekar, M. M.; Patil, V. S.; Gopinath, C. S.; Raja, T. Phase transfer ceria-supported nanocatalyst for nitrile hydration reaction. *ACS Omega* **2019**, *4*, 16037–16044.
[41] Wang, T.; Chen, W. C.; Liu, Q. D.; Wang, W.; Wang, Y. M.; Wu, B.; Shi, W. X.; Zhu, Y. Q.; He, P. L.; Wang, X. Self-assembly of polyoxometalate-based sub-1 nm polyhedral building blocks into rhombic dodecahedral superstructures. *Angew. Chem., Int. Ed.* **2023**, *62*, e202314045.
[42] Ha, Y.; Fei, B.; Yan, X. X.; Xu, H. B.; Chen, Z. L.; Shi, L. X.; Fu, M. S.; Xu, W.; Wu, R. B. Atomically dispersed co-pyridinic N-C for superior oxygen reduction reaction. *Adv. Energy Mater.* **2020**, *10*, 2002592.
[43] Li, Y. H.; Cai, X. H.; Chen, S. J.; Zhang, H.; Zhang, K. H. L.; Hong, J. Q.; Chen, B. H.; Kuo, D. H.; Wang, W. J. Highly dispersed metal carbide on ZIF-derived pyridinic-N-doped carbon for CO_2 enrichment and selective hydrogenation. *ChemSusChem* **2018**, *11*, 1040–1047.
[44] Liu, Y. X.; Wang, H. H.; Zhao, T. J.; Zhang, B.; Su, H.; Xue, Z. H.; Li, X. H.; Chen, J. S. Schottky barrier induced coupled interface of electron-rich N-doped carbon and electron-deficient Cu: In-built Lewis acid-base pairs for highly efficient CO_2 fixation. *J. Am. Chem. Soc.* **2019**, *141*, 38–41.
[45] Liang, J.; Wu, Q.; Huang, Y. B.; Cao, R. Reticular frameworks and their derived materials for CO_2 conversion by thermo-catalysis. *EnergyChem* **2021**, *3*, 100064.
[46] Chen, Y. M.; Chen, L. Y.; Li, Y. W.; Shen, K. Metal-organic frameworks as a new platform to construct ordered mesoporous Ce-based oxides for efficient CO_2 fixation under ambient conditions. *Small* **2023**, *19*, 2303235.